

DEVELOPMENT OF MAXIMUM POWER POINT TRACKING PLATFORM FOR PHOTOVOLTAIC SYSTEM

Tine Andrejašič, Marko Jankovec, Marko Topič

University of Ljubljana, Faculty of Electrical Engineering, Ljubljana, Slovenia

Key words: Maximum Power Point Tracking, high efficiency non-inverting buck-boost DC-DC Converter, photovoltaic system output maximization

Abstract: This paper describes a development of a prototype of Maximum Power Point Tracking platform for Photovoltaic Systems which is used for testing maximum power point tracking algorithms for different electric loads and to analyze the behavior of photovoltaic (PV) generator at different load regime during monitoring. The platform is composed of a power transfer circuit and periphery with microcontroller, signal acquisition and communication. The main part of the power circuit is designed as a high efficiency non-inverting buck-boost direct current-to-direct current (DC-DC) converter that enables power transfer of up to 400 W. Separate buck DC-DC converter is integrated to power all employed integrated circuits. Both current and voltage are measured at the input and output of the platform. FLASH program memory based microcontroller is used to apply integrated maximum power point algorithms and to control and harmonize the entire periphery. For simple communication between a computer and the platform's microcontroller a RS-485 based protocol was used with user interface developed in a graphical programming language LabVIEW.

Razvoj platforme za sledenje točke največje moči pri fotonapetostnih sistemih

Ključne besede: sledenje točke največje moči, DC-DC pretvornik z visoko učinkovitostjo pretvorbe, maksimiranje izhodne moči fotonapetostnega sistema

Izveček: Članek opisuje razvoj prototipa platforme za sledenje točke največje moči fotonapetostnega generatorja, ki služi testiranju učinkovitosti algoritmov in preučevanju delovanja fotonapetostnih modulov pri različnih obremenitvah. Sistem je sestavljen iz glavnega DC-DC stikalnega pretvornika, ki skrbi za prenos energije iz fotonapetostnega generatorja na breme in periferije, ki jo sestavlja mikrokrmilnik, vezje za zajemanje in merjenje signalov in komunikacijsko vezje. Glavni DC-DC stikalni pretvornik deluje v vezavi neinvertirajočega pretvornika navzgor-navzdol (izhodna napetost je lahko nižja ali višja od vhodne napetosti) z visoko stopnjo učinkovitosti pretvorbe za moči do 400 W. Sekundarni DC-DC stikalni pretvornik skrbi za napajanje vseh potrebnih integriranih vezij, ki delujejo na nizkem napetostnem nivoju. Platforma omogoča meritve toka in napetosti tako na vhodu kot tudi na izhodu sistema. Mikrokrmilnik skrbi za izvajanje implementiranih algoritmov iskanja in sledenja točke največje moči ter usklajuje delovanje ostale periferije. Za enostavno komunikacijo platforme z osebnim računalnikom smo izdelali tudi uporabniški vmesnik v programskem jeziku LabVIEW, ki deluje na podlagi protokola RS-485.

1. Introduction

Sustainable energy sources like PV solar systems are becoming important as eco-friendly alternatives to fossil fuels. Research and development efforts together with economy of scale in the photovoltaics lead to decreasing costs and strengthen implementation of different solar powered systems. Photovoltaic solar powered industrial applications include among others water pumping, air conditioning, electric vehicles and ventilation systems (predominantly acting as dynamic loads).

PV generator has a specific output characteristic. Output current-voltage (I - V) and power-voltage (P - V) characteristics of Phaesun 25 Wp poly-Si PV module under different solar irradiances in the plane of array (G_{p0a}) and cell temperatures are shown in Fig. 1 and Fig. 2.

In P - V characteristics P_{MPP} designates the power at the maximum power point (MPP).

As seen in Fig. 1, short circuit current (I_{sc}) and open circuit voltage (V_{oc}) are irradiance and temperature dependent. I_{sc} is linearly proportional to the solar irradiance, while the V_{oc} shows logarithmic dependence to irradiance. Since PV generators are still the most expensive part of the PV sys-

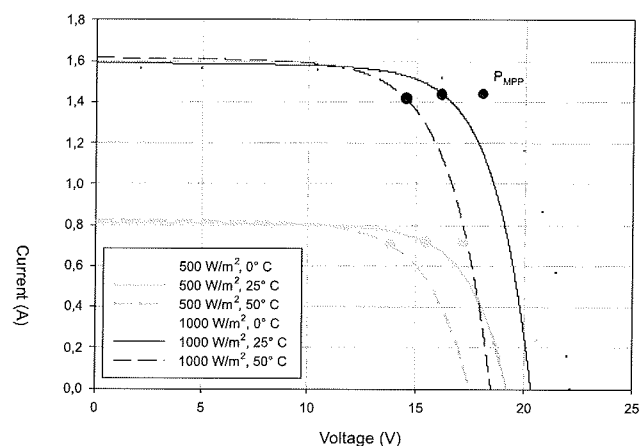


Fig. 1: Measured I - V photovoltaic panel characteristics for different solar irradiances in plane of array and cell temperatures.

tem, they must be loaded optimally to maximize conversion efficiency and decrease costs, size and weight. System should always operate in the P_{MPP} regardless instantaneous circumstances and temporal changes, such as solar irradiance, ambient temperature or any other ambient parameter. To achieve operation of the PV generator near the vicinity of the P_{MPP} with its specific value of voltage and

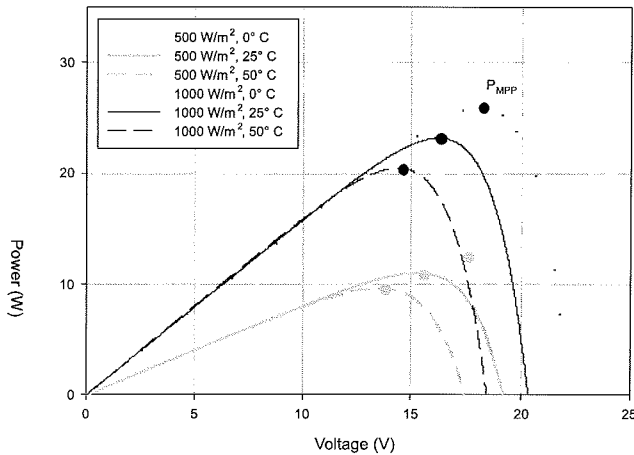


Fig. 2: Measured P-V photovoltaic characteristics for different solar irradiances in plane of array and cell temperatures.

current, switching mode pulse-width modulation (PWM) DC-DC converter /1/ must be inserted between the PV generator and electric load. The converter's primary task is to continuously adapt to the load and to track the instantaneous maximum power point of the PV generator.

Many MPP tracking algorithms for the DC-DC converters have been developed in the last decades. Recently, reviews of direct/indirect methods were presented in /2/ and /3/. Five of several direct methods have been implemented in our system.

2. Development of MPPT platform

High-efficiency maximum power point tracking (MPPT) system that could be connected to majority of PV modules available on the market and would act as a testing platform for maximum power point tracking algorithms was impossible to buy, so we had to develop it ourselves. Different MPPT algorithms are to be implemented and their performance compared while optimally regulating the power transferred to the load for different scenarios. Output voltage and current range should be high enough for battery powered system loads of voltages 48 V and below.

On the basis of those requirements we designed and built a microcontroller based maximum power point tracking platform that is comprised of a main DC-DC switching converter in buck/boost configuration, a low output voltage buck DC-DC converter, a voltage and current sensing circuit, a microcontroller and a communication circuit (Fig. 3).

The main converter continuously adapts the load impedance to track the instantaneous maximum power point of the PV generator or regulates constant output voltage in its regime. Input and output voltage range is from 0 to 60 V and maximum input and output currents are 8 A. The buck DC-DC converter is used to convert the applied voltage down to 7,5 V to power the main DC-DC converter regula-

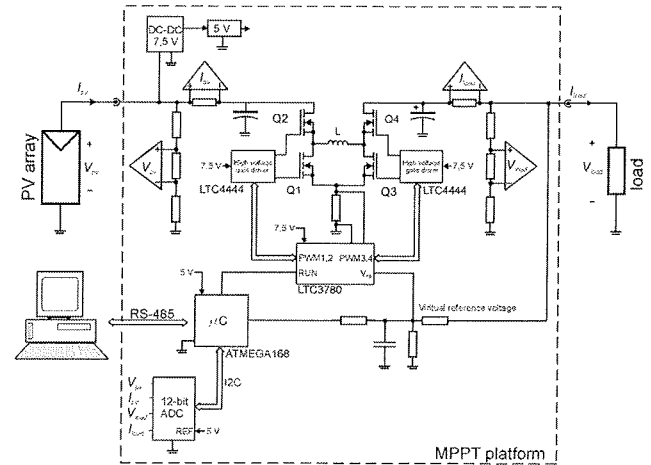


Fig. 3: Block diagram of maximum power point tracking platform.

tor, high voltage gate drivers and voltage sensing amplifiers. Linear regulator is added with an output voltage of 5 V to power the microcontroller, the AD converter and the communication circuit.

Output voltage, input voltage and current are filtered and scaled down for the input range of the analog-to-digital (AD) converter. ATMEGA168 microcontroller /4/ is used to communicate with the user interface and to harmonize the platform operation. It communicates with AD converter via I2C protocol to receive digitalized measurements that are required to execute maximum power point tracking algorithms. Microcontroller is able to set/reset the main regulator, set its feedback voltage and switch between continuous, discontinuous and burst mode of operation. For communication between the computer and microcontroller a RS-485 based protocol was used with user interface developed in a graphical programming language LabVIEW. It allows a user to choose between maximum power point algorithms and their parameters, set constant output voltage and track all measurable quantities.

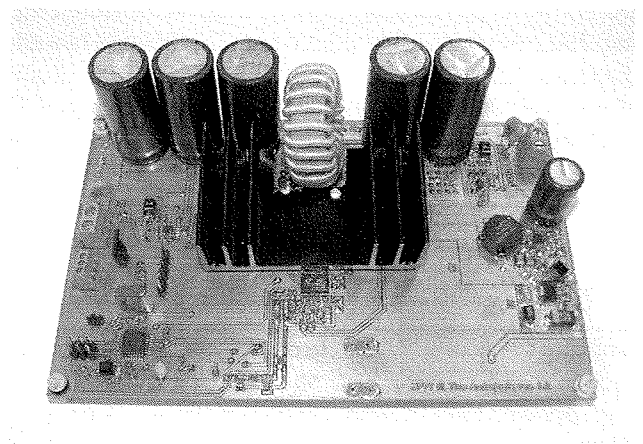


Fig. 4: Prototype of maximum power point tracking platform.

2.1 Buck/boost converter

Main DC-DC switching converter's task is to deliver as much power as possible from the connected PV generator to the load applied. Buck and boost topology were joined together in this converter regulated by LTC3780 /5/ current mode controller that provides an output voltage above, equal to or below the input voltage. It consists of four MOSFET switches in bridge configuration, inductor, input and output capacitors. If the input voltage is lower than output voltage the system works as a boost converter. MOSFET transistor Q2 stays on, while transistor Q1 stays off. Output is determined by pulse width modulation (PWM) signal applied to transistors Q3 and Q4. Every ten cycles Q1 and Q2 invert for 300 ns to charge Q2's bootstrap capacitor. When input voltage is near the output voltage, PWM signal is applied to all four switches. Converter operates in buck mode when the output voltage is lower than the input voltage. PWM signal is applied to transistors Q1 and Q2, transistor Q4 stays open and transistor Q3 is closed except for Q4's bootstrap capacitor recharging period every ten cycles. Output voltage is determined with feedback voltage by voltage divider circuit. To actively control the output voltage by microcontroller additional current is forced via RC circuit to the feedback voltage. Virtual feedback voltage sets the output voltage to its maximum (60 V), if no current is forced from microcontroller, and to 0 V when maximum current is forced.

Maximum input/output voltage rating for LTC3780 to safely operate is 36 V. To increase this voltage up to 60 V we inserted high voltage gate drivers LTC4444 /6/ on both output and input side of the converter.

2.2 Signal measurement

All direct maximum power point algorithms operate based on measured information from input or output power quantities. Implemented algorithms require both input and output signal measurements.

Main switching DC-DC converter and low voltage level DC-DC converter produce high level of noise in measured signal. The main converter operates at 200 kHz and has additional glitches every ten cycles at 20 kHz when bootstrap capacitors are charged. Low voltage level DC-DC converter works at 60 to 150 kHz according to the output current. Due to the noise and glitches in measured signals a lot of effort was invested to optimize signal measurement.

Input and output current measurement is implemented as measurement of voltage drop across high tolerance resistor. For this purpose high voltage high side operational amplifier LTC6101 /7/ was used to avoid common mode problems. To maintain high efficiency, resistors with low resistance and Kelvin connection were chosen. A low-pass filter was inserted between the AD converter and output of the amplifier.

Input and output voltage is measured on voltage divider (see Fig. 5).

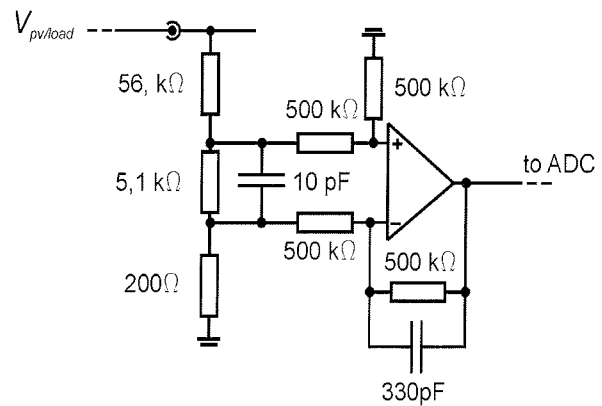


Fig. 5: Voltage measurement circuit.

Operation amplifier subtracts voltage across 5,1 kΩ resistor and adds a low-pass filter with cut-off frequency of 1 kHz. This kind of configuration eliminates majority of glitches and AC component in the signal. To filter the entire AC component in the signal lower cut-off frequency should be chosen, but this would affect regulation frequency of applied algorithms. That is the reason to implement additional weighted average digital filtering with a microcontroller.

MOSFET temperature is also monitored to ensure power-down when the heat dissipation is too high or at malfunction.

2. Conversion efficiency

Conversion efficiency as an important steady-state performance parameter was measured at input voltage of typical PV modules maximum power point voltage (V_{MPP}) of 16,1 V (12 V system), 28,5 V (24 V system) and representative of grid - tied module with V_{MPP} of 43,1 V. Output voltage was set to typical battery powered system voltages of 12, 24, 36 and 48 V. As we can observe from Fig. 6 to 9, the conversion efficiency drops at increasing ratio between input and output voltage and at increasing load currents.

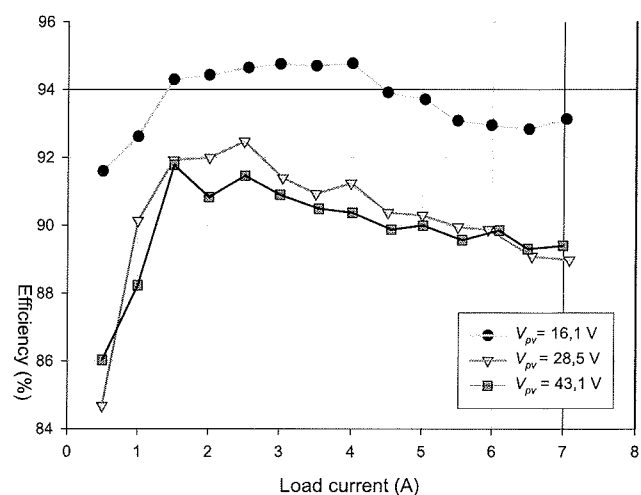


Fig. 6: Conversion efficiency at $V_{load} = 12 V$.

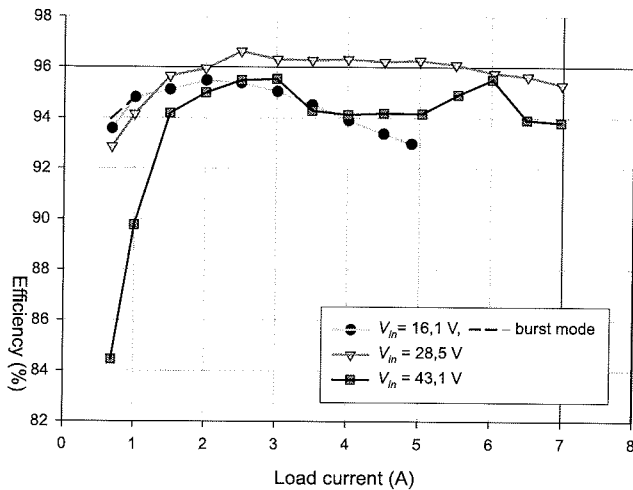


Fig. 7: Conversion efficiency at $V_{load} = 24 V$.

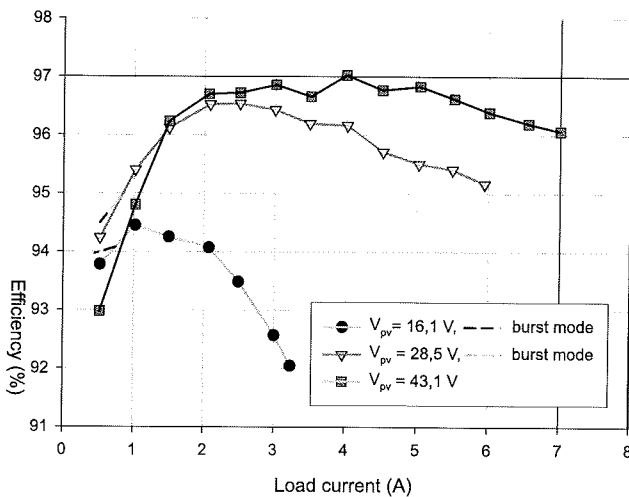


Fig. 8: Conversion efficiency at $V_{load} = 36 V$.

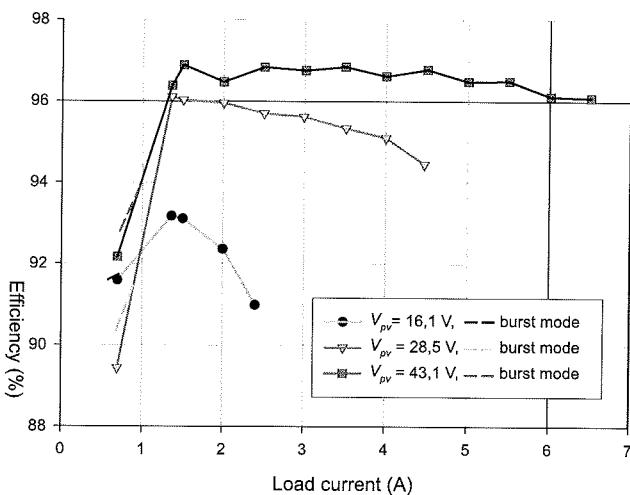


Fig. 9: Conversion efficiency at $V_{load} = 48 V$.

A comparison of forced continuous switching mode and burst switching mode operation was made to determine higher efficiency conversion at higher load currents. Reg-

ulator introduces higher level of feedback hysteresis in burst mode and produces output signals to the MOSFETs Q3 and Q4 that turns them on for several cycles, followed by a variable "sleep" interval depending upon the load current. In boost operation at higher load currents burst mode is more appropriate and results in improved efficiency by few percents.

The major sources of power loss in the converter are the switching losses of the MOSFETs, the inductor, the DC-DC low voltage converter and the I^2R losses on current-sensing resistors and power traces on circuit board. It is difficult to further improve the efficiency over the whole interval of operation. Selected intervals of operation with component specific values should be chosen to further optimize the efficiency.

3. Implemented MPPT algorithms

Indirect MPPT algorithms, such as look-up table based, fuzzy logic and neural network MPPT algorithms were not implemented in platform mainly because they depend on previous PV characterization and self teaching process /8/, /9/. Among direct seeking algorithms, *input* and *output Hill-Climbing (H-C)*, *Perturbe and Observe (P&O)*, *Incremental Conductance (IncCond)* and *Derivative dP/dt* have been implemented in the platform. Let us shortly review their principles and properties.

H-C algorithms have been investigated by several authors /2/, /3/, /10/, where MPP is tracked by changing the duty-cycle ratio of a DC-DC converter. Power is determined in each cycle by measuring current and/or voltage at the input or output side of the converter. If the power has increased after duty-cycle ratio change, the algorithm will continue in the same direction in the next cycle, otherwise the direction of duty-cycle ratio will be reversed. Both power and direction of duty-cycle ratio change have to be stored for each iteration. *H-C input* algorithm maximizes output power by sensing at the input side (PV generator), while *H-C output* maximizes power measured on the load.

Next type of algorithm is *Perturbe and Observe (P&O)* /2/, /3/, /11/. The *P&O* algorithms are widely used because of their simple structure. They operate by periodically perturbing (i.e. incrementing or decrementing) the PV generator terminal voltage and comparing the output power with that of the previous perturbation cycle. If the power is increasing, the perturbation will continue in the same direction in the next cycle, otherwise the perturbation direction will be reversed. In every perturbation PV generator reference voltage (V_{ref}) is calculated. This means the PV generator terminal voltage is regulated in every perturbation cycle by separate voltage regulating loop. Therefore when the MPP is reached, the *P&O* algorithm will oscillate around it.

An example of applied *P&O* algorithm for increased irradiance from $500 W/m^2$ to $800 W/m^2$ is presented in Fig. 9

at constant ambient temperature (T_{air}), 100 Hz regulating frequency of perturbation and 50 mV discrete step of V_{ref} . Initially the algorithm stabilized the maximum power point tracker at the maximum power for 500 W/m² irradiance. New level of irradiance (800 W/m²) was applied step-wise and presents the most dynamic outdoor scenario. After increased irradiance the algorithm is changing V_{ref} towards the new maximum power point voltage. The jitter in the tracking path is a consequence of discrete reference voltage step. In this experiment the algorithm needed 1,2 s to reach the new maximum power point. The stabilization would be faster if the discrete step of V_{ref} was increased, however the fluctuation around the reached P_{MPP} would be greater. In reality such rapid changes of irradiance are generally not expected therefore a faster tracking is not required. Results from different scenarios demonstrate that the algorithm with given parameters is capable of tracking irradiance changes up to 250 W/m² per second.

2D Graph 3

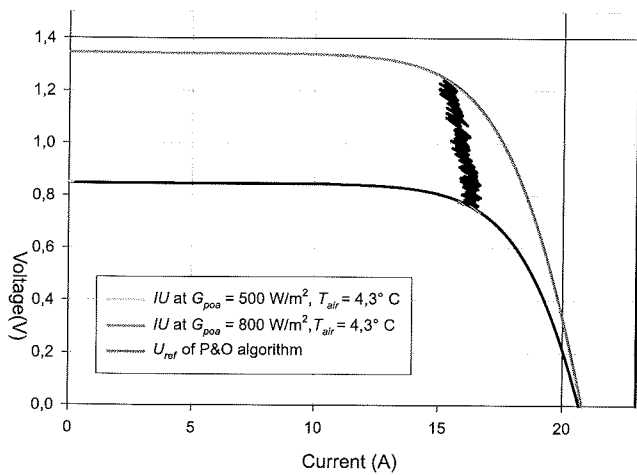


Fig. 10: Maximum power point tracking of P&O algorithm.

IncCond algorithm that measures and compares incremental and instantaneous conductance for rapidly changing ambient conditions was implemented in /2/, /3/, /12/ to increase tracking speed and lower the oscillations at steady conditions. Condition of maximum power $dP_{PV}/dV_{PV} = 0$ in (1) leads to (2), where the left side of the equation represents instantaneous conductance I_{PV}/V_{PV} , while its right side represents incremental conductance, determined by " I_{PV} and " V_{PV} as difference between values of the current and present cycle.

$$\frac{dP_{PV}}{dV_{PV}} = I_{PV} \frac{dV_{PV}}{dV_{PV}} + V_{PV} \frac{dI_{PV}}{dV_{PV}} = I_{PV} + V_{PV} \frac{dI_{PV}}{dV_{PV}} = 0 \quad (1)$$

$$\frac{I_{PV}}{V_{PV}} = -\frac{dI_{PV}}{dV_{PV}} \approx -\frac{\Delta I_{PV}}{\Delta V_{PV}} \quad (2)$$

The *IncCond* algorithm predicts in what direction the reference voltage should change to match the change of ambient conditions. If dP_{PV}/dV_{PV} is less than zero the PV generator is operating at voltage higher than voltage in P_{MPP}

(V_{MPP}) (see Fig. 2), otherwise it operates at voltage lower than V_{MPP} . Like in the P&O algorithms, a separate voltage high-speed regulating loop must be applied to regulate PV generator output voltage $V_{PV} \approx V_{ref}$.

The last algorithm that we have implemented is *derivative dP/dt* algorithm /13/. When PV generator operates at the MPP, the equations (3) and (4) must be fulfilled. MPP is reached by forcing its derivative dP/dt to zero under the power feedback control.

$$\frac{dP_{PV}}{dt} = \frac{d(I_{PV}V_{PV})}{dt} = V_{PV} \frac{dI_{PV}}{dt} + I_{PV} \frac{dV_{PV}}{dt} = 0 \quad (3)$$

$$VdI = -IdV \Rightarrow V\Delta I = -I\Delta V \quad (4)$$

If $-I\Delta V$ is less than $V\Delta I$, PV generator operates in voltage source mode ($V > V_{MPP}$, see Fig. 1) and the PV generator voltage must decrease, otherwise it operates in current source mode ($V < V_{MPP}$) and the generator voltage must increase to reach MPP. A separate voltage regulating loop is used to control PV generator output voltage.

The platform allows a user to implement and evaluate additional direct algorithms.

4. Conclusions

A maximum power point tracking platform has been successfully developed. Its wide input voltage and current range enable connection of majority of PV modules available on the market. The platform's conversion efficiencies are above 96% for broad range of output voltages and loads. The developed platform opens a route to implement and examine several direct MPPT algorithms along with sensitivity study of their parameters according to the given PV module, load characteristics and nature of changing of ambient conditions. Since PV generators are still the most expensive part of the PV systems, this could path the way to further maximize their conversion efficiency.

5. References:

- /1/ A.I. Pressman, *Switching Power Supply Design*, 2nd ed., New York: McGraw-Hill, 1998, pp. 32-35.
- /2/ T. Esmar, P.L. Chapman, *Comparison of Photovoltaic Array Maximum Power Point Tracking Techniques*, IEEE Transactions on Energy Conversion, Vol. 22, pp. 439-449, (2007),.
- /3/ V. Salas, E. Olias, A. Barrado, A. Lázaro, *Review of the Maximum Power Point Tracking Algorithms for Stand-alone Photovoltaics Systems*, Solar Energy Materials & Solar Cells Vol. 90, pp. 1555-1578, (2006).
- /4/ Web site for ATMEGA168 microcontroller, datasheet <http://www.atmel.com/dyn/resources/prod_documents/doc2545.pdf>, accessed on 05/08/2008.
- /5/ Web site for LTC3780 DC-DC buck/boost converter regulator, datasheet <<http://www.linear.com/pc/downloadDocument.do?navId=H0,C1,C1003,C1042,C1116,P10090,D7197>>, accessed on 01/09/2008.
- /6/ Web site for LTC4444 high voltage gate driver, datasheet <<http://www.linear.com/pc/downloadDocument.do?navId=H0,C1,C1003,C1142,C1041,P39339,D25652>>, accessed on 11/09/2008.

- /7/ Web site for LTC6101 high side, high voltage current sense amplifier, datasheet <<http://www.linear.com/pc/downloadDocument.do?navId=H0,C1,C1154,C1009,C1077,P10220,D7277>>, accessed on 02/09/2008.
- /8/ N. Mutoh, T. Matuo, K. Okada, M. Sakai, Prediction-data-based maximum-power-point-tracking method for photovoltaic power generation systems, Proc. 33rd Annu. IEEE Power Electron. Spec. Conf., pp. 1489-1494, (2002).
- /9/ I.H. Altas, A.M. Sharaf, A novel maximum power fuzzy logic controller for photovoltaic solar energy systems, Renewable Energy, Vol. 33, p.p. 388-399, (2008).
- /10/ N. Dasgupta, A. Pandey, A.K. Murkerjee, Voltage-sensing-based Photovoltaic MPPT with Improved Tracking and Drift Avoidance Capabilities, Solar Energy Materials & Solar Cells, Vol. 92, pp. 1552-1558, (2008).
- /11/ D. Shmilovitz, Photovoltaic Maximum Power Tracking Employing Load Parameters, IEEE Proc. ISIE, Dubrovnik, Croatia, (2005), pp. 1037-1042.
- /12/ K. H. Husein, I. Muta, T. Hoshino, M. Osakada, Maximum power tracking: an algorithm for rapidly changing atmospheric conditions, IEE Proc. Gener. Transm. Distrib, Vol. 142pp. 59-64, (1995).
- /13/ C. Kunlun, Z. Zhengming, Y. Liqiang, Implementation of Stand-alone Photovoltaic Pumping System with Maximum Power Point Tracking, Electrical Machines and Systems, ICEMS Proc., Vol. 1, pp. 612-615, (2001).

*Tine Andrejašič, univ. dipl. ing. el.
Dr. Marko Jankovec, univ. dipl. ing. el.
Prof. Dr. Marko Topič, univ. dipl. ing. el.*

*University of Ljubljana,
Faculty of Electrical Engineering,
Laboratory of Photovoltaics and Optoelectronics,
Tržaška cesta 25, SI-1000 Ljubljana, Slovenia*

E-mail: tine.andrejasic@fe.uni-lj.si

Prispelo (Arrived): 10.03.2009 Sprejeto (Accepted): 09.09.2009